Materials Letters: X 18 (2023) 100190

Contents lists available at ScienceDirect

Materials Letters: X

journal homepage: www.sciencedirect.com/journal/materials-letters-x

Investigations on tailoring physical properties of RF magnetron sputtered Cadmium Sulphide thin films

Harshita Trivedi [a], Zohreh Ghorannevis [b], Shilpi Chaudhary [c,*], Avanish S. Parmar [a,*]

[a] Department of Physics, Indian Institute of Technology (BHU), Varanasi, India
[b] Department of Physics, Karaj Branch, Islamic Azad University, Karaj, Iran
[c] Department of Applied Sciences, Punjab Engineering College (Deemed to be University), Chandigarh, India

ARTICLE INFO

Keywords:
CdS
RF sputtering
Thin-films
Optical properties
N_2 concentration

ABSTRACT

The effect of nitrogen (N_2) partial pressure on the structure and bandgap tunability of RF magnetron sputtered Cadmium Sulphide (CdS) thin films is investigated by varying N_2 partial pressure in Ar/N_2 mixture. In presence of N_2, films have a polycrystalline structure with (0 0 2) preferential orientation, which leads to defect-free, continuous, dense, and fibrous structures with increased roughness. The average optical transmittance increased to > 80 at 500–2500 nm for 30 % N_2 partial pressure, whereas the band gap decreases from 2.45 eV to 2.30 eV with increasing N_2 concentration. This work shows that the bandgap of sputtered CdS thin films can be tuned with the variation of N_2 concentration for customized applications.

1. Introduction

Semiconductor thin films play an important role in basic and industrial research, owing to their ability to control the electrical and optical properties. [1–3] Due to their significant optical transmission, cheaper cost, tunable bandgap, and high absorbance coefficient [4], CdS thin films have applications in optoelectronics, LED, transistor, and solar cells. [5–9] CdS thin films have been fabricated by various techniques including spray pyrolysis [10,11], Electrodeposition [12], pulsed laser deposition [13], sputtering [14], and thermal evaporation. [15] Among the other methods, RF magnetron sputtering can deposit the films at low temperatures with high coverage, better adhesion, and high film quality. Several studies have been performed to optimize factors such as bandgap, deposition time, and thickness to produce high-quality CdS thin films. The optical bandgap of CdS layer can be improved by thinning the CdS layer by forming alloys at either the cation (CdZnS) or anion (CdS:O) sites. [16].

Here, we have studied the influence of nitrogen (N_2) concentration in Ar/N_2 mixture on the bandgap tunability and structural variations of CdS thin films fabricated by RF magnetron sputtering. [17] Structural properties revealed that CdS thin films are homogeneous without defects, or voids, and have shown a polycrystalline structure in (0 0 2) preferential orientation. Thin films sputtered at a higher concentration of N_2 partial pressure with Ar/N_2 mixture have shown a decrease in optical bandgap by 0.15 eV than those fabricated with pure Ar gas. [18,19] The impact of changing the N_2/Ar sputtering ambient composition on the intrinsic properties of sputtered CdS films is quantified, which can be utilized as an n-type semiconductor layer in second-generation thin-film solar cells.

2. Experimental details

CdS thin films were synthesized via RF magnetron sputtering (Kurt J. Lesker Co) under controlled growth conditions with a variation of N_2 concentration (10% to 30% with a step size of 10% in Ar/N_2 mixture). The chamber was initially evacuated to a high vacuum of $8x10^{-6}$ Torr. The gas flow rate of sputtering gas Ar (99.99% purity) was set to 60 sccm and deposition time was 60 min. All samples were deposited in the same environment.

The phase identification and chemical compositions of fabricated sputtered films were examined by using XRD, (Stoe XPERT-PRO). The surface structures, morphology, and roughness of thin films were analyzed by FESEM, (Hitachi S4160) and AFM, (Solver Next, NT-MD).

3. Results and discussion

XRD spectra (Fig. 1) represents a body-centered cubic CdS structure with a preferential growth in the (0 0 2) direction. [20] The strength of

* Corresponding authors.
E-mail addresses: shilpichaudhary@pec.edu.in (S. Chaudhary), asparmar.phy@itbhu.ac.in (A.S. Parmar).

https://doi.org/10.1016/j.mlblux.2023.100190
Received 30 January 2023; Received in revised form 1 March 2023; Accepted 19 March 2023
Available online 25 March 2023

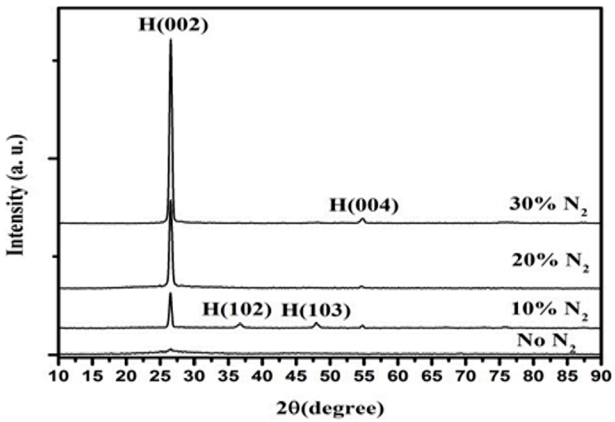

Sample	2θ (002)	B (radian)	D (nm)	ε×10^{-3}	δ×10^{-3} (nm)$^{-2}$
No N_2 (pure Ar)	26.62	0.0201	7.20	21.8	19.2
10% N_2 in Ar/ N_2 mixture	26.56	0.0061	23.43	6.72	1.82
20% N_2 in Ar/ N_2 mixture	26.61	0.0082	17.57	8.94	3.23
30% N_2 in Ar/ N_2 mixture	26.61	0.0082	17.57	8.94	3.23

Fig. 1. XRD pattern of sputtered CdS thin films and tabular summary of structural parameters for different N_2%.

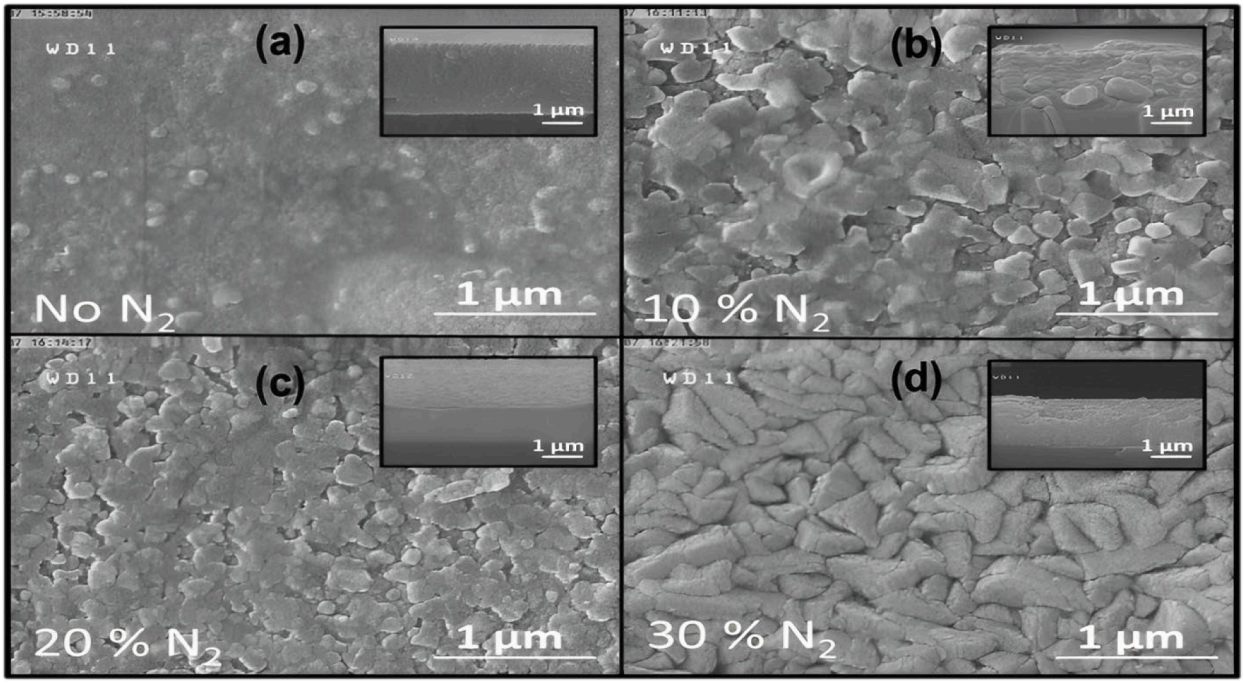

Fig. 2. FESEM images of sputtered CdS thin films at different N_2%.

significant peaks increases, indicating that crystallization along the corresponding direction is substantially better at higher N_2 concentrations without any changes in orientation preferences. Multiple diffraction peaks are observed at 10 % N_2 concentration.

Micro-strain and Dislocation density [21] of sputtered thin films are:

$$\varepsilon = \beta \cos(\theta)/4$$

$$\delta = n/D^2$$

where β is the full-width half-maximum (FWHM), ε is strain, and Bragg's angle is θ. D is the average crystallite size.

Scherer's equation was used to calculate the crystallite size. [22] A tabular summary (Fig. 1) is provided on dislocation density, grain size, and crystallite size for CdS thin films. Due to the higher N_2 flow rate, and the variation in the mean free path of molecules, the deposited molecules do not have sufficient mobility to settle down in a stable orientation. At higher nitrogen partial pressures, the fluctuation in the mean free route may lead the atoms to alter orientation during the development of thin film, resulting in a preferred orientation along (002). Furthermore, the reduction in surface energy may be one of the reasons for such an orientation shift. The crystallite size of a sputtered thin film deposited in Ar/N_2 environment is smaller in comparison to the film deposited in pure Ar; implying that the crystallite size of the sputtered film decreases in the presence of N_2. No discernible influence on the films' dislocation density or micro-strain with the addition of nitrogen.

The FESEM images (Fig. 2) of sputtered thin films show a variation of nitrogen concentration on surface morphologies and microstructures properties of the thin films. It has been reported that N_2 in films can be present from the residual gas and the working gases (Ar + N_2). [23] It can be observed from Fig. 2 (a-b) that the film surfaces have grassy and rough morphology. It can be noted that the film at higher N_2 concentration had a fibrous grain and fine valleys, Fig. 2 (c-d). The increase in N_2 concentration promotes a smoother surface. The fibrous grains were grown from the substrate to the surface, which provides good adhesion between the glass substrate and the bulk layer of thickness. Filled morphology without voids of spherical grain structures is achieved due to the generation of charge carriers during the reaction with N_2.

AFM analysis (Fig. 3) shows that films are consistent and homogeneous. The AFM pictures revealed that the surface is made up of small,

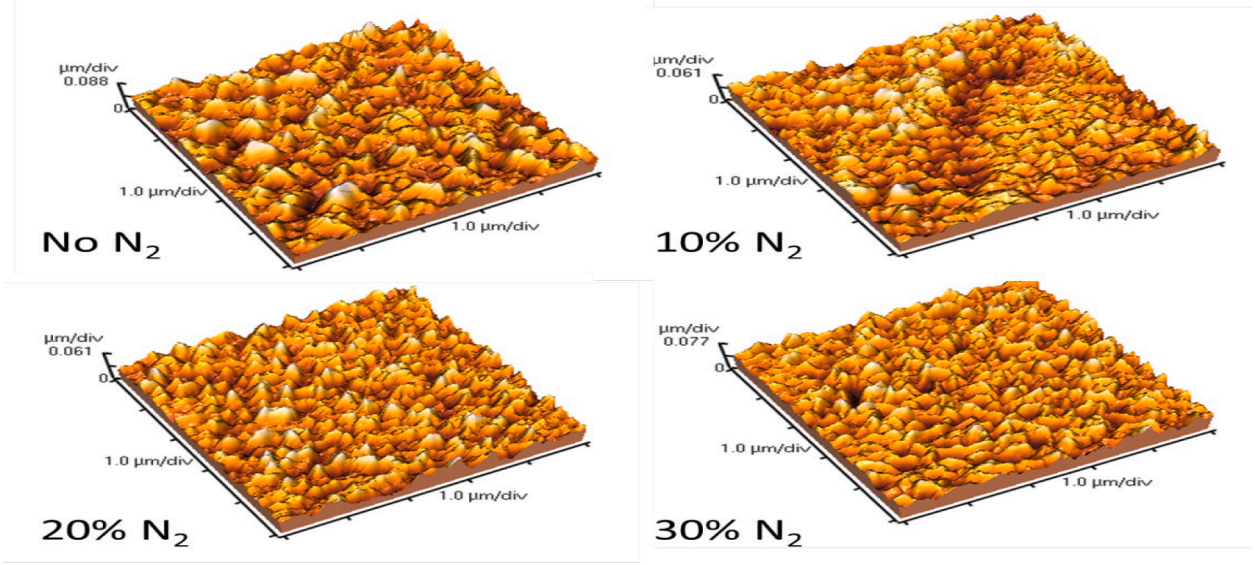

Fig. 3. AFM images of CdS thin films sputtered at different N_2%.

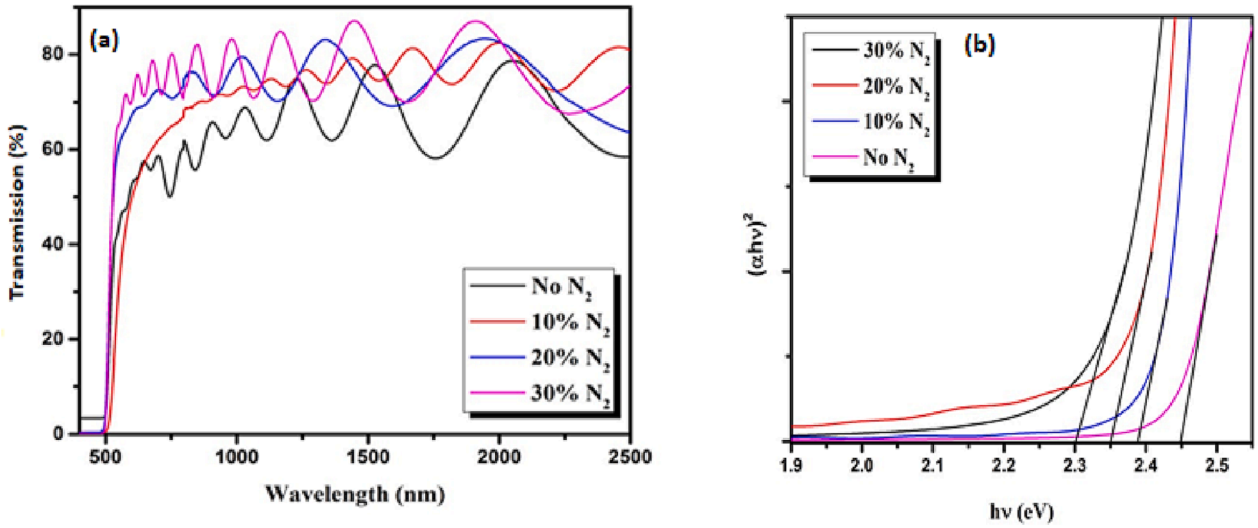

Fig. 4. (a) Transmission spectra (b) plot of $(\alpha h\upsilon)^2$ vs. photon energy for CdS thin films at different N_2%.

tightly packed, and homogeneous structures. The kinetic energy of sputtered CdS particles is lower at lower N_2 concentrations than at higher N_2 concentrations, resulting in more random orientation and various grain sizes, which leads to surface roughness. As the N_2 concentration rises, the kinetic energy (KE) of the CdS particles rises and bombardment with high KE particles can result in increased surface roughness. An increment of KE at intermediate N_2 concentration has decreased the roughness of the surface but increased again at higher N_2 concentration, attributed to the large coarse grain. An incremental rise of N_2 concentration leads to the destruction of the surface and the creation of voids and defects in the structure. Structural properties of CdS thin films deposited with 30 % N_2 are in remarkably good agreement with the FESEM and XRD spectra.

The transmittance spectra (Fig. 4) of CdS thin films at various N_2 concentrations in the Ar/ N_2 mixture were measured with the wavelength range 500–2500 nm by UV–Vis spectroscopy. Transmission spectra reveal that the average optical transmittance is $>$ 80%, which is appropriate for solar cells and other optoelectronic applications.[24] The structure of the film, which is influenced by different sample preparation techniques, film thickness, and deposition parameters, has a substantial impact on transmission. The presence of interference fringes in the visible region of transmittance spectra represents that sputtered CdS films have better crystallinity and small defect density near the band edge; whereas the presence of sharp absorption edges in the visible region of transmittance reveals that the films have a smooth surface, supporting the findings from FESEM.

The bandgaps were determined using the modified Tauc's method equation-

$$\alpha h\upsilon = A(h\upsilon - E_g)^{1/2}$$

where α is the absorption coefficient, hυ is the incident photon energy, A is constant, and Eg is the optical bandgap energy.

Fig. 4 (b) depicts the fluctuation of the optical bandgap as a function of N_2 concentration. The bandgap at pure Ar is about 2.45 eV. When N_2 concentration is increased by 10%, 20%, and 30% the bandgap reduces from 2.38 eV, 2.35 eV to 2.30 eV, respectively. These bandgap values were smaller than the bulk CdS band gap (2.42 eV). [25] Here, CdS can be an effective window material in different photovoltaic applications such as CdS/CdTe and CdS/Cu_2S solar cells because of its optimized

bandgap. [26].

4. Conclusion

To conclude, the effects of N_2 on the structural and optical properties of sputtered CdS thin films were investigated. The introduction of N_2 concentration in the Ar/ N_2 mixture during the deposition of CdS thin films changed their crystallinity and exacerbated their amorphous character, as confirmed by the XRD spectrum. FESEM and AFM analysis reveals the production of continuous, smooth, and dense films free of defects, vacancies such as cracks, and protrusion. The UV–visible absorption spectra revealed that the bandgap decreases significantly with the variation of N_2 content. With increased N_2 partial pressure, a significant increase in transmittance $>$ 80 at 500–2500 nm was observed. This work shows that by including N_2 in Ar gas during deposition, optical characteristics of sputtered CdS thin films can be tuned. CdS with such a narrow bandgap (2.30 eV) can be employed as window material in numerous optoelectronic device applications, such as solar cells.

CRediT authorship contribution statement

Harshita Trivedi: Conceptualization, Methodology. **Zohreh Ghorannevis:** Conceptualization. **Shilpi Chaudhary:** Writing – original draft. **Avanish S. Parmar:** Writing – review & editing, Supervision.

Declaration of Competing Interest

The authors declare that they have no known competing financial interests or personal relationships that could have appeared to influence the work reported in this paper.

Data availability

Data will be made available on request.

Acknowledgments

The authors would like to thank the Department of Science and Technology (DST-SERB), India- CRG/2019/000903 (Core Research Grant) & SB/S2/RJN-140/2014 (Ramanujan Fellowship Award). S. Chaudhary also acknowledges the grant from DST (SERB), for Start-up Research Grant, India- SRG/2020/000777.

References

[1] E. Sabbir, P. Chelvanathan, S. Ahmad, B. Bais, S. Kiong, K. Sopian, Sol. Energy 177 (2019) 262–273.
[2] Y. Lei, Z. Jiang, Z. Zhang, J. Mater. Sci. Mater. Electron. 29 (9) (2018) 7675–7680.
[3] M. Nakata, C. Zhao, J. Kanicki, Solid State Electron. 116 (2016) 22–29.
[4] S. Swathi, R. Yuvakkumar, G. Ravi, E.S. Babu, D. Velauthapillai, A. Syed, T.M. S. Dawoud, Appl. Nanosci. 10 (2020) 4351–4358.
[5] A. Giberti, et al., Sens. Actuators B 207 (2015) 504–510.
[6] R. Ansir, et al., Solid State Electron. 172 (2020), 107886.
[7] Zia, Riaz, M. Anjum, Optik 127 (2016) 5407–5412.
[8] P. Samir, K. Raval, J. Mater. Sci. Mater. Electron. 28 (2017) 18031–18039.
[9] J. Kwon, J. Ahn, H. Yang, Curr. Appl Phys. 13 (2013) 84–89.
[10] Shaikh, S.S. Shkir, M. Masumdar, Phys. B Condens. Matter 571 (2019) 64–70.
[11] E. Gavrishchuk, et al., Opt. Mater. 117 (2021), 111153.
[12] M. Aliyu, D.G. Diso, A.O. Musa, J. Abubakar, Pure Appl. Sci. 13 (2022) 539–545.
[13] B. Liu, et al., J. Alloy. Comp. 654 (2016) 333–339.
[14] S. Rondiya, et al., Thin Solid Films 631 (2017) 41–49.
[15] C. Dai, et al., J. Vac. Sci. Technol. A 10 (3) (1992) 484–488.
[16] I.O. Oladeji, et al., Sol. Energy Mater. Sol. Cells 61 (2) (2000) 203–211.
[17] P. Tirmali, et al., Solid State Electron. 62 (1) (2011) 44–47.
[18] E.C. Prima, et al., Opt. Mater. 114 (2021), 110947.
[19] I.M. El Radaf, T.A. Hameed, I. Yahia, Mater. Res. Express 5 (6) (2018), 066416.
[20] A.S. Najm, H.S. Naeem, et al., Coatings 12 (10) (2022) 1400.
[21] F.G. Hone, F.K. Ampong, Mater. Chem. Phys. 183 (2016) 320–325.
[22] M. Islam, et al., Thin Solid Films 546 (2013) 367–374.
[23] N. Das, et al., Results Phys. 17 (2020), 103132.
[24] A. Obaid, et al., Sol. Energy 89 (2013) 143–151.
[25] J.P. Enríquez, X. Mathew, Sol. Energy Mater. Sol. Cells 76 (3) (2003) 313–322.
[26] W. Zhou, et al., Appl. Surf. Sci. 255 (5) (2008) 2885–2889.